








Since January 2020 Elsevier has created a COVID-19 resource centre with free information in English and Mandarin on the novel coronavirus COVID-19. The COVID-19 resource centre is hosted on Elsevier Connect, the company's public news and information website.

Elsevier hereby grants permission to make all its COVID-19-related research that is available on the COVID-19 resource centre - including this research content - immediately available in PubMed Central and other publicly funded repositories, such as the WHO COVID database with rights for unrestricted research re-use and analyses in any form or by any means with acknowledgement of the original source. These permissions are granted for free by Elsevier for as long as the COVID-19 resource centre remains active.

ORIGINAL ARTICLE

von Willebrand factor in experimental malaria-associated acute respiratory distress syndrome

Sirima Kraisin¹ | Sebastien Verhenne¹ | Thao-Thy Pham² | Kimberly Martinod¹  |
 Claudia Tersteeg¹ | Nele Vandeputte¹ | Hans Deckmyn¹  | Karen Vanhoorelbeke¹  |
 Philippe E. Van den Steen²  | Simon F. De Meyer¹ 

¹Laboratory for Thrombosis Research, KU Leuven Campus Kulak Kortrijk, Kortrijk, Belgium

²Laboratory of Immunoparasitology, Rega Institute for Medical Research, KU Leuven, Leuven, Belgium

Correspondence

Simon F. De Meyer, Laboratory for Thrombosis Research, KU Leuven Campus Kulak Kortrijk, E. Sabbelaan 53, 8500 Kortrijk, Belgium.
 Email: simon.demeyer@kuleuven.be

Funding information

Research Foundation-Flanders, Grant/Award Number: G086215N and G070315; Research Fund, Grant/Award Number: C16/17/010; Horizon 2020 Marie Skłodowska-Curie Actions Individual Fellowship, Grant/Award Number: 747993

Abstract

Background: Malaria-associated acute respiratory distress syndrome (MA-ARDS) is a lethal complication of severe malaria, characterized by marked pulmonary inflammation. Patient studies have suggested a link between von Willebrand factor (VWF) and malaria severity.

Objectives: To investigate the role of VWF in the pathogenesis of experimental MA-ARDS.

Methods: *Plasmodium berghei* NK65-E (*PbNK65*) parasites were injected in $Vwf^{+/+}$ and $Vwf^{-/-}$ mice. Pathological parameters were assessed following infection.

Results: In accordance with patients with severe malaria, plasma VWF levels were increased and ADAMTS13 activity levels were reduced in experimental MA-ARDS. ADAMTS13- and plasmin-independent reductions of high molecular weight VWF multimers were observed at the end stage of disease. Thrombocytopenia was VWF-independent because it was observed in both $Vwf^{+/+}$ and $Vwf^{-/-}$ mice. Interestingly, $Vwf^{-/-}$ mice had a shorter survival time compared with $Vwf^{+/+}$ controls following *PbNK65* infection. Lung edema could not explain this shortened survival because alveolar protein levels in $Vwf^{-/-}$ mice were approximately two times lower than in $Vwf^{+/+}$ controls. Parasite load, on the other hand, was significantly increased in $Vwf^{-/-}$ mice compared with $Vwf^{+/+}$ mice in both peripheral blood and lung tissue. In addition, anemia was only observed in *PbNK65*-infected $Vwf^{-/-}$ mice. Of note, $Vwf^{-/-}$ mice presented with two times more reticulocytes, a preferential target of the parasites.

Conclusions: This study suggests that parasite load together with malarial anemia, rather than alveolar leakage, might contribute to shortened survival in *PbNK65*-infected $Vwf^{-/-}$ mice. VWF deficiency is associated with early reticulocytosis following *PbNK65* infection, which potentially explains the increase in parasite load.

KEYWORDS

malaria, *Plasmodium berghei* NK65, respiratory distress syndrome, reticulocytes, von Willebrand Factor

1 | INTRODUCTION

Malaria is a global health problem, leading to 219 million cases and 435 000 deaths in 2017.¹ One of the most lethal complications is malaria-associated acute respiratory distress syndrome (MA-ARDS). All human malarial parasites are able to cause MA-ARDS in patients, but the majority of cases are caused by *Plasmodium falciparum* and *Plasmodium vivax*.² MA-ARDS often develops during or after antimalarial treatment, and the mortality rate can reach up to 80%.³ The pathogenesis of MA-ARDS remains elusive, but involves inflammation-mediated alveolocapillary membrane permeability leading to diffuse alveolar damage, resulting in ventilation-perfusion mismatch and impaired gas exchange, which can persist and even aggravate after parasite clearance.⁴ In contrast to cerebral malaria, in which sequestration of infected red blood cells (iRBCs) is known to occur massively on the microvascular endothelium in the brain, little is known about the role of parasite sequestration in the pulmonary microvasculature.

In recent years, a pathogenic role for von Willebrand factor (VWF) activity in malaria has been suggested.⁵ VWF is a glycoprotein synthesized in endothelial cells (ECs) and megakaryocytes, playing a crucial role in normal hemostasis and thromboinflammation.^{6,7} VWF mediates the adhesion of platelets at sites of vascular injury and protects procoagulant factor VIII from early degradation in circulation.⁸ In addition, VWF also promotes leukocyte adhesion and inflammation.^{9,10} Endothelial VWF is either constitutively secreted into plasma as a series of heterogeneous multimers, or stored as ultralarge VWF (ULVWF) multimers in Weibel-Palade bodies.⁶ The adhesive activity of VWF is based on the size of its multimers. This multimeric size is regulated by the metalloproteinase ADAMTS13 (A Disintegrin And Metalloprotease with a ThromboSpondin type 1 motif, member 13), which cleaves VWF into smaller and consequently less thrombogenic forms.

Several studies have shown that during *P falciparum* infection, patients have increased levels of plasma VWF and decreased ADAMTS13 activity, which leads to the accumulation of circulating ULVWF multimers.¹¹⁻¹⁵ It has been suggested that spontaneous binding of platelets to ULVWF multimers might mediate thrombocytopenia, a common feature of patients infected with *P falciparum*.^{16,17} Furthermore, Bridges et al¹⁸ demonstrated that iRBCs are able to bind platelets that are attached to the ULVWF in a CD36-dependent manner, a phenomenon that could possibly facilitate sequestration and disease progression. Whether VWF is involved in MA-ARDS is currently unknown. In this study, we used an established mouse model of MA-ARDS to specifically address the putative roles of VWF in this malarial lung complication. In this mouse model, infection with *Plasmodium berghei* NK65-E (*PbNK65*) does not cause experimental cerebral malaria, but leads to pulmonary inflammation with protein-rich interstitial and alveolar edema, which becomes lethal typically between 8 and 11 days postinfection (PI).^{4,19,20}

Essentials

- Patient studies have suggested a link between von Willebrand Factor (VWF) and malaria severity.
- We studied VWF in experimental malaria-associated acute respiratory distress syndrome.
- VWF contributed to increased alveolar leakage.
- VWF deficiency was associated with elevated parasite load, anemia, and shortened survival time.

2 | MATERIALS AND METHODS

2.1 | Mice

VWF knockout (*Vwf*^{-/-}) and wild-type (*Vwf*^{+/+}) mice were on a C57BL/6J background and were initially obtained from the Jackson Laboratory (Bar Harbor, ME). Characterization of *Vwf*^{-/-} mice has been described previously.²¹ Plasminogen knockout (*Plasminogen*^{-/-}) and wild-type (*Plasminogen*^{+/+}) mice were on a C57BL/6J background (kind gift from Professor Francis Castellino, The University of Notre Dame, Notre Dame, IN). All experiments were performed on mice of 6-8 weeks of age of both sexes. Different groups of mice in each experiment were age-, sex-, and weight-matched. Mice showing signs of moribundity (i.e., severely reduced activity, lethargy, respiratory distress) were considered to have reached a humane endpoint and euthanized by cervical dislocation according to ethical guidelines. All mouse experiments were performed in accordance with protocols approved by the Institutional Animal Care and Use Committee of KU Leuven, Belgium. This study was approved under project number P173/2015.

2.2 | Parasite infection

C57BL/6J mice infected with *PbNK65* parasites (a kind gift from the late D. Walliker, University of Edinburgh, Scotland, UK) were used as a mouse model of MA-ARDS. The characterization of this model has been previously described.^{19,20} To grow parasites, two *Vwf*^{+/+} C57BL/6J mice were intraperitoneally injected with a frozen stock of infected blood. When parasitemia levels were between 3% and 5%, tail blood was diluted in Dulbecco's phosphate buffered saline, and 10⁴ iRBCs were injected intraperitoneally in experimental mice. Drinking water of infected and control mice was supplemented with 0.375 mg/mL p-aminobenzoic acid for optimal growth of parasites.

2.3 | Parasitemia

Thin blood smears obtained from 2 μ L of tail vein bleeds were made and stained with Giemsa solution (1/10 dilution; Sigma-Aldrich, St. Louis, MO). The percentage of iRBCs in peripheral blood (parasitemia) was determined by microscopical analysis.

2.4 | Blood collection

Mice were anesthetized with 5% isoflurane (Nicholas Piramal Limited, London, UK) in 100% O₂. Blood samples were collected by retro-orbital puncture into 0.5 mol/L ethylenediaminetetraacetic acid (1 volume to 40 volumes of blood) or 3.8% trisodium citrate (1 volume to 6 volumes of blood). Complete blood counts were obtained from ethylenediaminetetraacetic acid-anticoagulated blood using a Hemavet 950FS Multi-Species Hematology system (Drew Scientific, Oxford, CT). Plasma samples were prepared from citrated blood by centrifugation at 4300 × g for 6 minutes and stored at -80°C until analysis.

2.5 | VWF antigen and multimers

VWF antigen (VWF:Ag) levels and VWF multimer patterns were performed as described previously.^{22,23}

2.6 | ADAMTS13 antigen and activity

ADAMTS13 antigen (ADAMTS13:Ag) levels were determined via enzyme-linked immunosorbent assay as described²⁴ with small modifications. Briefly, a 96-well microtiter plate was coated overnight with 5 µg/mL of the in-house developed monoclonal anti-mouse ADAMTS13 (mADAMTS13) antibody 14H7B8. After blocking with 3% milk powder solution, plasma samples were added in the wells. Captured mADAMTS13 was detected with an in-house developed polyclonal rabbit anti-mADAMTS13 antibody at a concentration of 5 µg/mL. Horseradish peroxidase-labeled goat anti-rabbit antibody (Jackson ImmunoResearch Laboratories Inc., West Grove, PA) was used to detect the bound antibody. The coloring reaction was induced by adding ortho-phenylenediamine substrate together with H₂O₂, and then stopped with 4 mol/L H₂SO₄. Absorbance was read at 490 nm.

ADAMTS13 activity (ADAMTS13:Act) levels were determined using the fluorescent resonance energy transfer substrate-VWF73 assay (Peptides International; Louisville, KY) as described previously.²⁵

2.7 | ADAMTS13 activity inhibition

In-house developed monoclonal antibodies (mAbs) against mADAMTS13 were used to inject in *Pb*NK65-infected *Vwf*^{+/+} mice. Five days after the infection, the mice were injected with either a combination of inhibitory mAbs 13B4 and 14H7 (2.50 mg/kg; 1.25 mg/kg each), or noninhibitory mAb 20A10 (2.50 mg/kg). The characterization of these mAbs was described previously.²⁴ ADAMTS13 activity levels in plasma were measured after mAbs injection using the fluorescent resonance energy transfer substrate assay.²⁴

2.8 | Plasmin-α2-antiplasmin complex determination

Levels of plasmin-α2-antiplasmin complex were measured as described previously.^{26,27} Briefly, a microtiter plate was coated with

polyclonal rabbit antibodies against mouse α2-antiplasmin. Diluted plasma samples were applied and incubated overnight. Captured plasmin-α2-antiplasmin complexes were detected with horseradish peroxidase-conjugated polyclonal rabbit anti-murine plasminogen antibodies against mouse plasminogen. Fully activated murine plasma with 50 nmol/L of urokinase plasminogen activator for 90 minutes at 37°C was used for calibration.

2.9 | Protein concentration in bronchoalveolar lavage

To collect bronchoalveolar lavage (BAL) fluids, mice were anesthetized by administering a ketamine/xylazine mixture (up to 100 mg/kg body weight ketamine and 16 mg/kg body weight xylazine) via intraperitoneal injection. Once the mice reached a surgical plane of anesthesia, BAL fluids were harvested from the lungs by intratracheal instillation of 750 µL sterile phosphate buffered saline (PBS) through a trachea cannula. This was performed twice, and the combined lavages were centrifuged (10 minutes at 335 × g, 4°C).⁴ Protein concentrations of the supernatants were determined by Bradford assay. Briefly, supernatants were diluted in PBS (1:2 dilution series) and mixed with Coomassie Plus reagent (Thermo Scientific, Rockford, IL). The absorbance was read at 570 nm. Serial dilutions of bovine serum albumin were used to make a standard curve. Mice that were dissected for the collection of BAL fluids were not included in the survival analysis.

2.10 | Parasite accumulation in the lungs determined by quantitative reverse transcription-polymerase chain reaction

After mechanical homogenization of the left lung, total RNA was extracted (RNeasy mini kit; Qiagen, Hilden, Germany) and quantified (Nanodrop; Thermo Fisher, Aalst, Belgium), complementary DNA (cDNA) was synthesized (High capacity cDNA reverse transcription kit; Thermo Fisher), and quantitative reverse transcription-polymerase chain reaction was performed on 25 and 12.5 ng cDNA. *P. berghei* (*Pb*) 18S RNA was determined with the following primer and probe sets, synthesized by Integrated DNA Technologies (IDT, Leuven, Belgium): TAA CAT GGC TTT GAC GGG TAA (forward primer), TGC TGC CTT CCT TAG ATG TG (reverse primer) and TCC GGA GAG GGA GCC TGA GAA ATA (probe). *Pb* 18S RNA data were normalized to the corresponding expression of the murine 18S RNA.²⁸ Mice that were dissected for the lung isolation were not included in the survival analysis.

2.11 | Reticulocyte quantification

To quantify reticulocytes, tail vein blood samples were obtained, and approximately 2 × 10⁶ red blood cells (RBCs) were diluted in 100 µL of 2% of fetal calf serum in Dulbecco's phosphate buffered saline. Cells were stained at 4°C with APC/Cy7-conjugated anti-TER119 (116223; Biolegend, San Diego, CA) and Brilliant Violet 421-conjugated anti-CD71 (113813; Biolegend) antibodies for 20 minutes. After washing steps, the samples were analyzed using a BD FACSVerser flow

cytometer (BD Biosciences, San Jose, CA) in conjunction with BD FACSuite Software. Percent reticulocytes (TER119⁺/CD71^{hi}) were calculated as the percentage of the total RBC population (TER119⁺).

2.12 | Statistics

All statistical analysis was performed using GraphPad Prism software (Prism version 5.04 for Windows; La Jolla, CA). Statistical differences between two groups were assessed by using Mann-Whitney *U* test or *t* tests (two-tailed) based on the normal distribution test (D'Agostino-Pearson normality test). Survival data were analyzed using a log-rank (Mantel-Cox) test. All data were expressed as means \pm standard error of the mean. Values of $P < 0.05$ were considered statistically significant.

3 | RESULTS

3.1 | *PbNK65* infection leads to increased VWF antigen and decreased ADAMTS13 activity levels in plasma

To investigate the role of VWF in MA-ARDS pathogenesis, we used an established mouse model of MA-ARDS, in which C57BL/6J mice are infected with *PbNK65*.¹⁹ Parasites in the peripheral circulation were occasionally detectable on blood smears at day 3 PI and further increased gradually over the course of the infection (Figure 1A). Concurrent with patient studies, increased levels of plasma VWF:Ag were seen in our MA-ARDS model (Figure 1B). Although only a few numbers of iRBCs appeared on blood smears

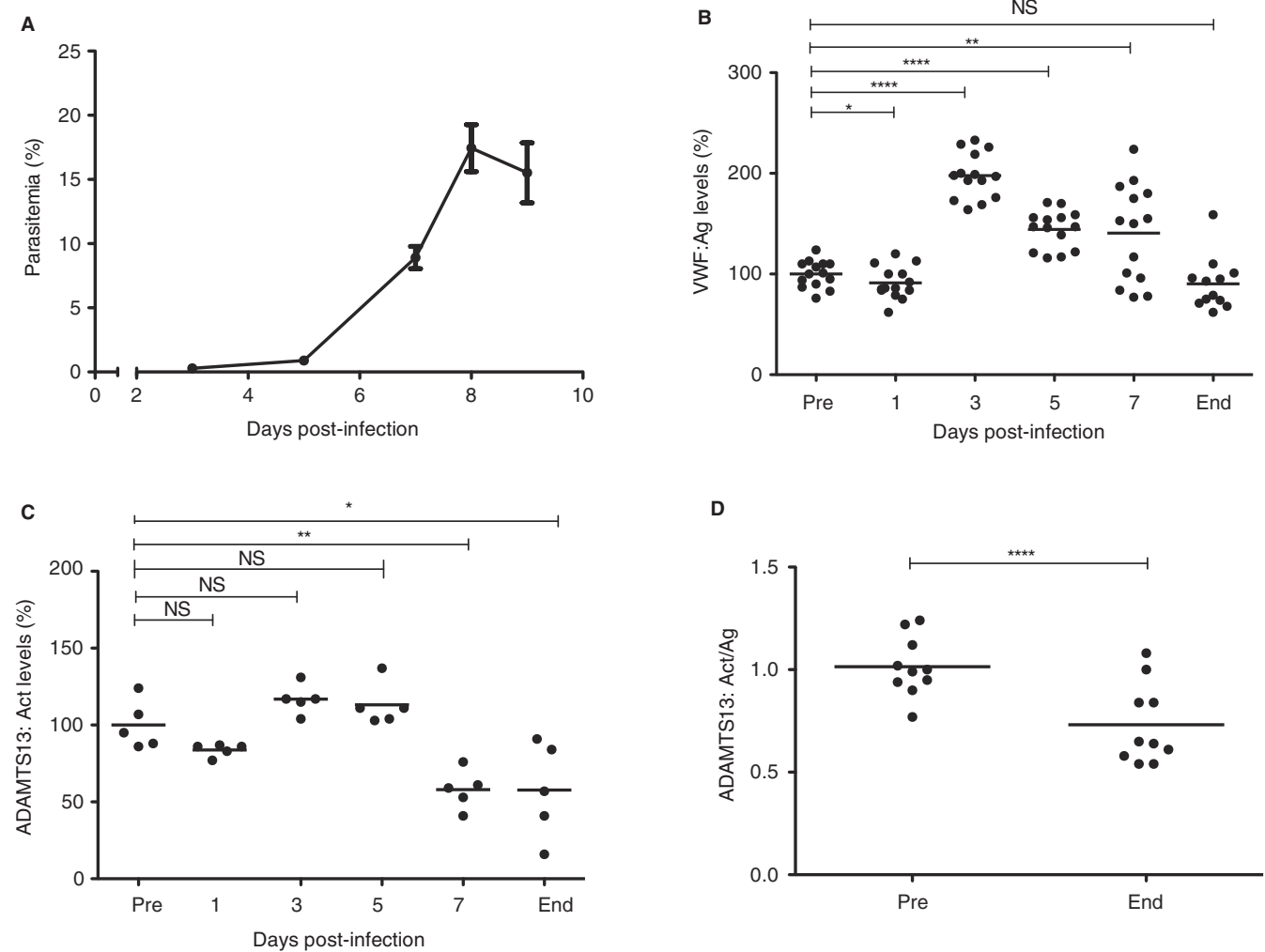


FIGURE 1 Early increased plasma VWF levels and late-stage reduction of ADAMTS13 activity levels during *PbNK65* infection. *Vwf*^{+/+} C57BL/6J mice were infected by intraperitoneal injection of 10^4 *PbNK65* parasites. Blood samples were collected 2 weeks before infection (pre) and at indicated time points after infection. Final blood samples were withdrawn at the end stage of disease (end) (i.e., when the mice were considered moribund [8–9 days PI]). A, Peripheral parasitemia levels were determined from Giemsa-stained blood smears. B, Plasma VWF:Ag levels were measured by enzyme-linked immunosorbent assay. C, Plasma ADAMTS13:Act were assessed using fluorescent resonance energy transfer substrate-VWF73 assay. D, To measure both ADAMTS13:Act and ADAMTS13:Ag before infection and at the end stage of disease, a separate group of *Vwf*^{+/+} C57BL/6J mice was infected with *PbNK65* parasites. Individual levels of ADAMTS13:Act and ADAMTS13:Ag are shown in Figure S1 and the ratio is given in panel D. Results represent the mean \pm standard error of the mean (* $P < 0.05$, ** $P < 0.01$, **** $P < 0.0001$, NS, Not significant. PI, postinfection; VWF, von Willebrand factor; VWF:Ag, von Willebrand factor antigen)

3 days PI, plasma VWF:Ag levels were already significantly increased compared with preinfection values ($197.8 \pm 6.0\%$ vs $100.0 \pm 3.5\%$, $P < 0.0001$) (Figure 1B). Furthermore, we observed a significant reduction of plasma ADAMTS13:Act levels in the late stage of infection at day 7 and 8/9 PI compared with baseline controls ($58.0 \pm 5.7\%$ and $57.8 \pm 13.8\%$ vs $100.0 \pm 7.0\%$, $P < 0.01$ and $P < 0.05$, respectively) (Figure 1C). To investigate whether these decreased activity levels resulted from reduced protein concentration, ADAMTS13:Ag and ADAMTS13:Act were measured in a separate experiment in which plasma samples were collected before infection and at the end stage of disease (8 or 9 days PI, when the mice were considered moribund, Figure S1). Interestingly, reductions of ADAMTS13:Act levels occurred independently of ADAMTS13:Ag levels (Figure S1), resulting in a significant reduction of ADAMTS13:Act to ADAMTS13:Ag ratio ($P < 0.0001$) (Figure 1D).

3.2 | *PbNK65* infection causes an ADAMTS13-independent reduction of high molecular weight VWF multimers

In addition to plasma VWF levels, VWF multimer composition was also analyzed in this MA-ARDS model. ULVWF multimers, which have a size larger than high molecular weight (HMW) VWF multimers, were not visible on the multimer gels. However, the amount of HMW VWF multimers at the end stage of disease was two times lower compared with PBS-injected controls ($48.0 \pm 2.0\%$ in PBS vs $19.8 \pm 2.3\%$ in *PbNK65*, $P < 0.0001$) (Figure 2A, B). These reduced fractions of HMW VWF multimers were independent of ADAMTS13 activity because similar reductions were also observed upon inhibition of ADAMTS13 by inhibitory anti-ADAMTS13 mAbs ($41.4 \pm 2.0\%$ in baseline controls vs $23.1 \pm 2.8\%$ in end-stage samples, $P = 0.013$) (Figure S2).

Plasmin has been suggested to cleave VWF in the absence of ADAMTS13^{29,30}; therefore, we measured plasmin generation in plasma of *PbNK65*-infected mice. Plasmin was highly generated at day 7 PI and at the end stage of disease (7-fold increase compared with baseline values $P < 0.01$) (Figure S3A). However, plasmin is not responsible for the reductions of HMW VWF multimers at the end stage of disease because similar reductions were observed in *Plasminogen*^{-/-} mice infected with *PbNK65* parasites (Figure S3B, C). Thus, the mechanism underlying the reductions of circulating HMW VWF multimers following *PbNK65* infection remains unclear, but is independent of ADAMTS13 and plasmin.

3.3 | VWF deficiency shortens survival in experimental MA-ARDS regardless of alveolar edema

To determine whether the elevated level of plasma VWF in this MA-ARDS model was simply a biomarker of EC activation, or whether VWF was directly implicated in the pathogenesis of MA-ARDS, we studied *PbNK65* infection in *Vwf*^{-/-} mice compared with *Vwf*^{+/+} controls. Both groups were infected with *PbNK65* parasites and were monitored daily. Interestingly, survival time was slightly but significantly shortened in *Vwf*^{-/-} mice compared with *Vwf*^{+/+} controls ($P = 0.003$) (Figure 3A). Nine days PI, approximately 70% of *Vwf*^{+/+} mice were still alive compared with only 20% in *Vwf*^{-/-} mice.

MA-ARDS is characterized by the disruption of the alveolar-capillary membrane integrity, leading to leakage of plasma fluid in the interstitium and the alveoli, resulting in alveolar edema. To assess alveolar edema, BAL fluids were collected in the morning of day 8 PI and protein levels were measured. Interestingly, total protein levels in *Vwf*^{-/-} mice were two times lower than those observed in *Vwf*^{+/+} mice (1.9 ± 0.3 vs 3.8 ± 0.5 mg/mL, respectively, $P < 0.01$) (Figure 3B). In summary, these data indicate that although VWF deficiency is

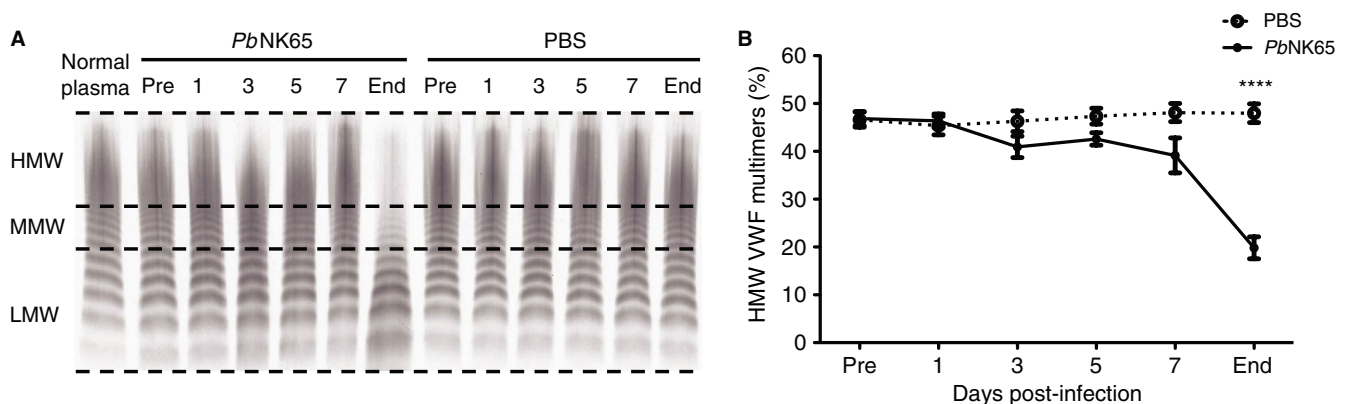


FIGURE 2 *PbNK65* infection is associated with loss of high molecular weight VWF multimers at end stage of disease. During the course of *PbNK65* infection, blood samples were collected from *Vwf*^{+/+} mice 2 weeks before infection (pre), at indicated days PI, and at the end-stage of disease (end) (i.e., when the mice were considered moribund [8-9 days PI]). Plasma VWF multimer compositions were assessed by agarose gel electrophoresis and densitometry. A, Representative VWF multimer distribution of a *PbNK65*-infected mouse and PBS control is shown. B, VWF multimer compositions were analyzed via densitometry. Relative abundance of HMW multimers is presented ($n = 8$ in *PbNK65*-infected group and $n = 4$ in PBS controls). Results represent the mean \pm standard error of the mean (**** $P < 0.0001$). HMW, high molecular weight (bands >10); LMW, low molecular weight (bands 1-5); MMW, medium molecular weight (bands 6-10); PI, postinfection; VWF, von Willebrand factor

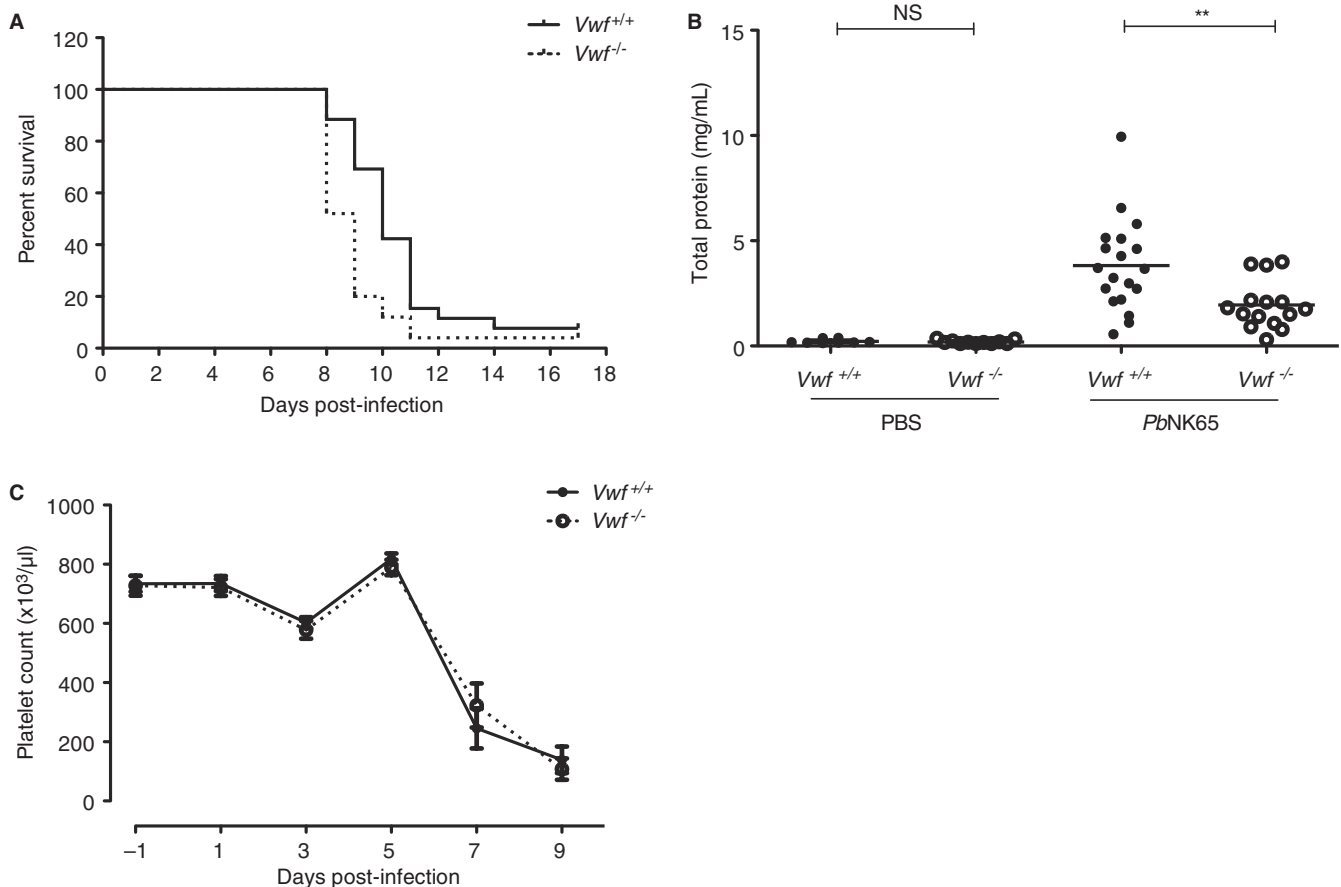


FIGURE 3 Survival time is shortened in VWF-deficient mice, regardless of lung edema and platelet count. *Vwf^{+/+}* and *Vwf^{-/-}* mice were infected with 10^4 *PbNK65*-infected red blood cells. **A**, Overall survival of *PbNK65*-infected *Vwf^{+/+}* ($n = 26$) and *Vwf^{-/-}* ($n = 25$) mice was determined and analyzed by log-rank (Mantel-Cox) test. This was significantly shortened in *Vwf^{-/-}* mice compared with *Vwf^{+/+}* controls ($P = 0.003$). **B**, Bronchoalveolar lavage fluids were harvested at day 8 PI, and protein concentrations were measured to determine alveolar leakage. PBS-injected mice were used as controls. **C**, Blood samples were taken from *PbNK65*-infected *Vwf^{+/+}* ($n = 12$) and *Vwf^{-/-}* ($n = 14$) mice at specified time points. Platelet counts were measured using an automated cell counter. Results represent the mean values \pm standard error of the mean (** $P < 0.01$). PI, postinfection; PBS, phosphate buffered saline; VWF, von Willebrand factor

associated with reduced alveolar leakage, *Vwf^{-/-}* mice nevertheless have a reduced survival in experimental MA-ARDS.

3.4 | Thrombocytopenia in experimental MA-ARDS is independent of VWF

Thrombocytopenia is a common symptom in patients with *P. falciparum* infection,³¹ in which VWF has been proposed to contribute.^{16,17,32} To investigate potential mechanisms underlying shortened survival in *Vwf^{-/-}* mice, platelet counts were measured in *Vwf^{+/+}* and *Vwf^{-/-}* mice over the course of *PbNK65* infection. In line with patient studies, severe thrombocytopenia was also observed in our MA-ARDS model (Figure 3C). Mean platelet count in *PbNK65*-infected *Vwf^{+/+}* mice dropped from $734 \pm 26 \times 10^3$ platelets/ μL before the infection, to $245 \pm 67 \times 10^3$ platelets/ μL at day 7 PI ($P < 0.0001$). Interestingly, *Vwf^{-/-}* mice also developed similarly severe thrombocytopenia following *PbNK65* infection ($737 \pm 37 \times 10^3$ platelets/ μL before the infection, to $230 \pm 56 \times 10^3$ platelets/ μL at day 7 PI) (Figure 3C).

Thrombocytopenia is therefore clearly independent of VWF in experimental MA-ARDS.

3.5 | VWF-deficient mice develop increased parasite load and anemia

To further investigate the mechanisms through which *Vwf^{-/-}* mice had a shorter survival time than *Vwf^{+/+}* mice following *PbNK65* infection, peripheral parasitemia levels and parasite accumulation in lung tissue were assessed. Parasitemia levels were markedly increased in *Vwf^{-/-}* mice compared with *Vwf^{+/+}* controls (Figure 4A). At day 7 PI, parasitemia reached $11.4 \pm 1.1\%$ in *Vwf^{+/+}* mice, whereas levels of $23.5 \pm 2.1\%$ were observed in *Vwf^{-/-}* mice ($P < 0.0001$). In line with parasitemia levels, parasite accumulation in the lungs harvested at the beginning of day 8 PI was also significantly elevated in *Vwf^{-/-}* mice compared with *Vwf^{+/+}* controls ($P < 0.001$) (Figure 4B). In addition to increased parasite loads, *Vwf^{-/-}* mice developed anemia at day 8 PI, as shown by decreased hemoglobin levels compared with *Vwf^{+/+}* mice (9.6 ± 0.7 vs 12.6 ± 0.4 mg/mL, $P < 0.01$) (Figure 4C).

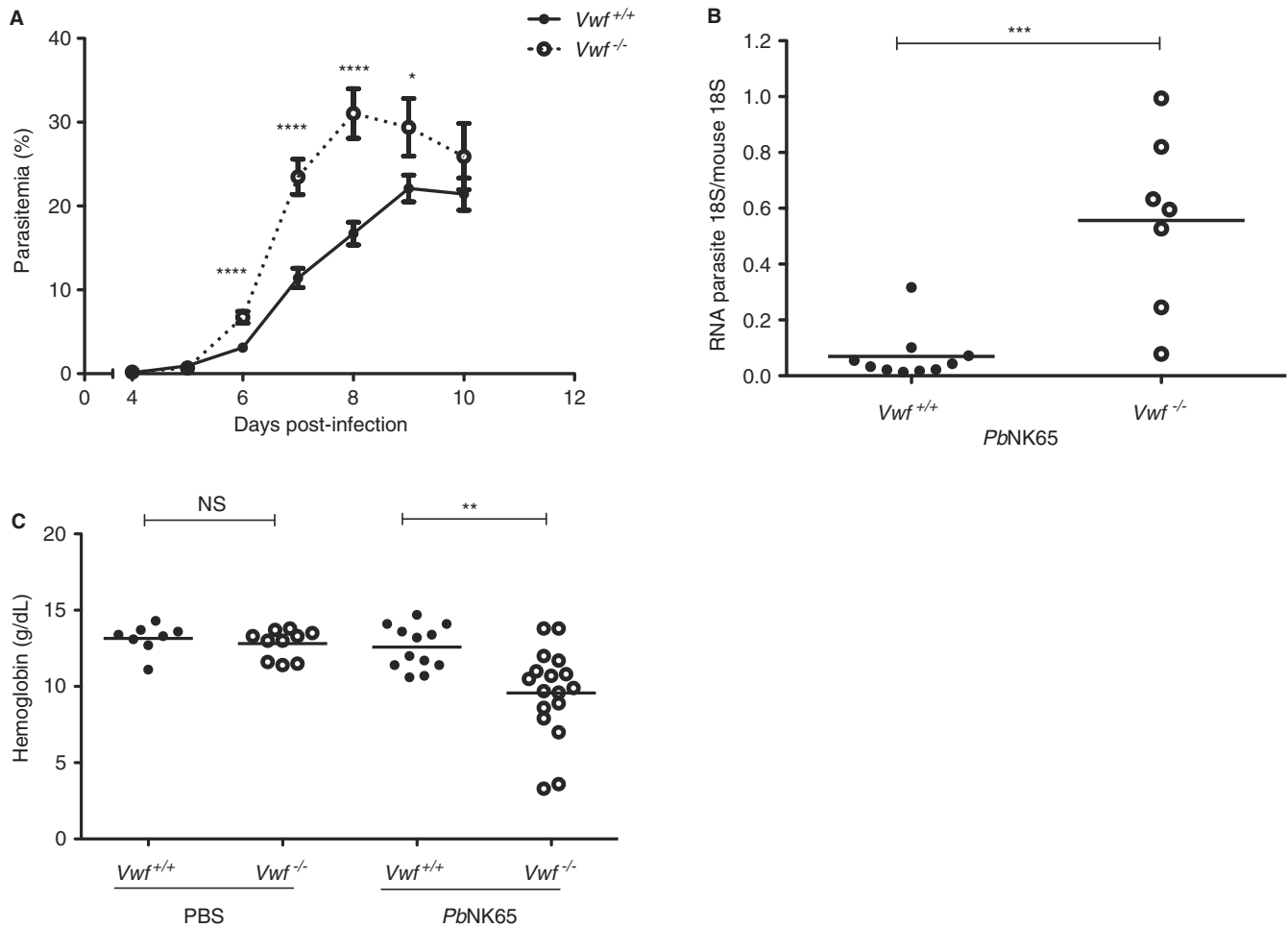


FIGURE 4 VWF-deficient mice are associated with increased parasite load. Parasitemia and parasite accumulation in the lungs were assessed following *PbNK65* infection. A, Peripheral parasitemia levels as determined from Giemsa-stained blood smears in both $Vwf^{+/+}$ ($n = 26$) and $Vwf^{-/-}$ ($n = 25$) mice. B, Parasite loads in perfused lungs harvested 8 days PI were determined by quantifying parasite 18S RNA transcripts compared with mouse 18S RNA transcripts. C, Blood samples were taken 8 days PI and hemoglobin levels were measured using an automated cell counter. Results represent the mean values \pm standard error of the mean (* $P < 0.05$, ** $P < 0.01$, *** $P < 0.001$, **** $P < 0.0001$). PI, postinfection; VWF, von Willebrand factor

Altogether, these data show that $Vwf^{-/-}$ mice have shortened survival time following *PbNK65* infection, presumably via increased parasite loads in both peripheral blood and lung tissue.

3.6 | VWF deficiency is associated with increased reticulocyte counts following *PbNK65* infection

Pberghei is known to have a predilection for invading reticulocytes (immature RBCs) over mature RBCs.^{20,33,34} Considering that parasitemia levels may vary because of the difference in reticulocyte numbers, RBC morphology in blood smears over the course of *PbNK65* infection was therefore taken into account. Remarkably, we noticed that peripheral blood smears of $Vwf^{-/-}$ mice taken before 7 days PI, when circulating iRBCs were markedly increased, contained at least two times more reticulocytes than those from $Vwf^{+/+}$ controls (Figure 5A). We therefore quantified the reticulocyte numbers in *PbNK65*-infected $Vwf^{+/+}$ and $Vwf^{-/-}$ mice via flow cytometry (gating strategy is shown in Figure S4). Although no differences in reticulocyte numbers

between $Vwf^{+/+}$ and $Vwf^{-/-}$ mice were seen at baseline, reticulocyte production was significantly increased in $Vwf^{-/-}$ mice compared with $Vwf^{+/+}$ mice after *PbNK65* inoculation (Figure 5B). At day 3 PI reticulocyte counts in $Vwf^{-/-}$ mice were twice as high of those in $Vwf^{+/+}$ mice ($5.6 \pm 1.3\%$ vs $2.6 \pm 0.6\%$, $P < 0.05$, respectively), which is prior to the prominent appearance of parasites on blood smears (Figure 5B). Because rodent reticulocytes circulate in the bloodstream for approximately 1 day and *PbNK65* parasites have the asexual blood-stage lifecycle of 1 day,^{35,36} we looked for a correlation between reticulocyte numbers and next day parasitemia levels. Reticulocyte numbers at day 5 PI were strongly correlated to the parasitemia levels at day 6 PI ($r^2 = 0.7$, $P < 0.0001$), the day at which the difference in parasitemia levels became significant (Figure 5C). A similar correlation was also seen between reticulocyte numbers 6 days PI and parasitemia levels 7 days PI ($r^2 = 0.2$, $P < 0.01$, data not shown). Altogether, these data indicate that increased parasitemia levels and parasite accumulation in the lungs of *PbNK65*-infected $Vwf^{-/-}$ mice, might be explained by the elevated number of reticulocytes at earlier time points.

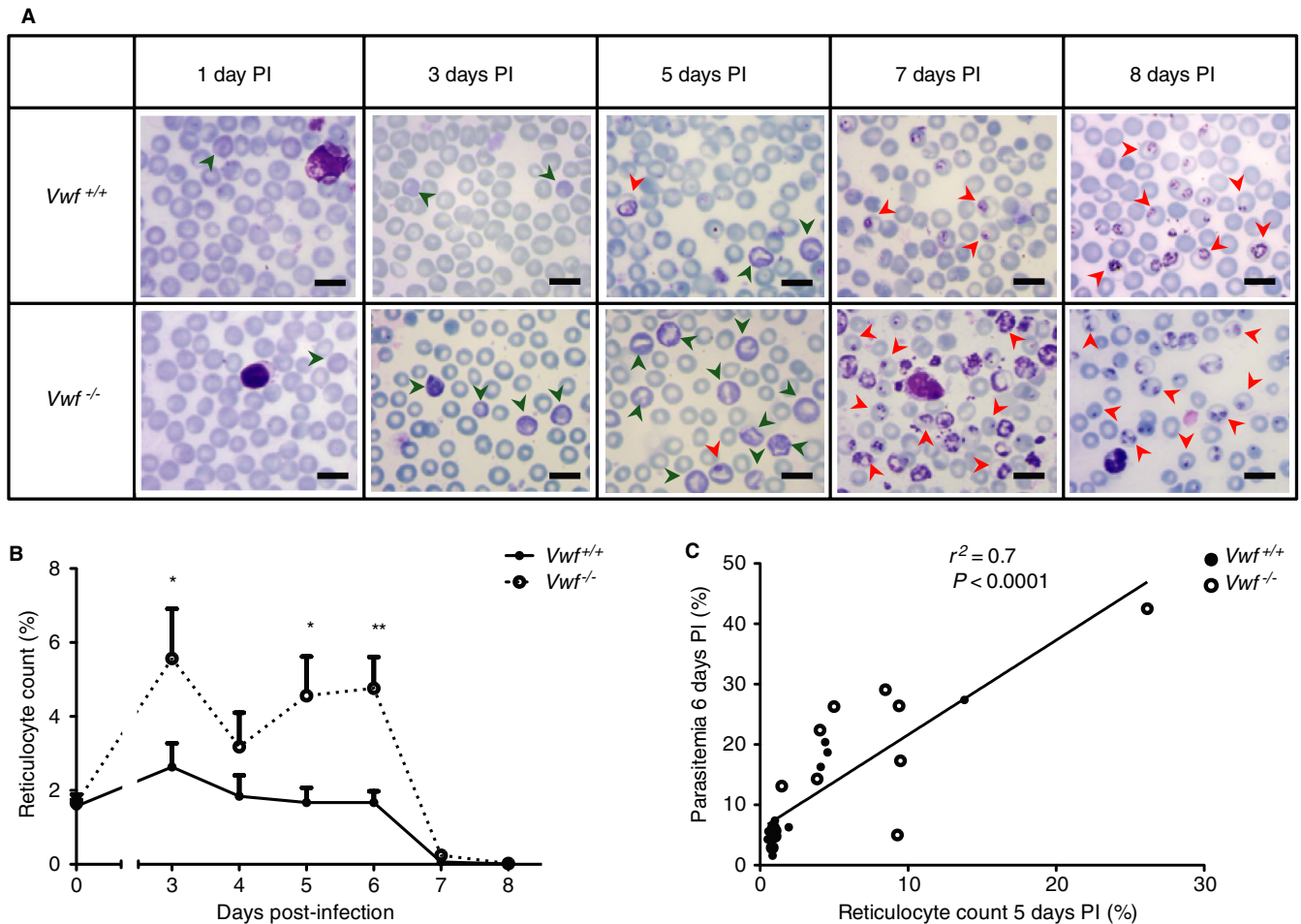


FIGURE 5 VWF deficiency is associated with reticulocytosis leading to increased parasitemia levels. *Vwf*^{+/+} (n = 15) and *Vwf*^{-/-} mice (n = 13) were infected with *PbNK65* parasites. Reticulocyte numbers and parasitemia were monitored daily. A, Representative microscopy images of Giemsa-stained blood smears are shown (original magnification, 100 \times ; scale bars, 5 μ m). Reticulocytes (green arrowheads) and examples of iRBCs (red arrowheads) are evident. B, Percentages of reticulocytes (TER119⁺/CD71^{Hi}) in the total number of erythrocytes (TER119⁺) were measured at the indicated time points using flow cytometry. C, Spearman correlations were determined between parasitemia levels at day 6 PI and reticulocyte numbers at day 5 PI. Results represent the mean values \pm standard error of the mean (* P < 0.05, and ** P < 0.01). iRBC, infected red blood cell; PI, postinfection; VWF, von Willebrand factor;

4 | DISCUSSION

In this study, we have unraveled the role of VWF in MA-ARDS pathogenesis by using an established mouse model. In this model, mice develop severe lung pathology symptoms similar to patients without any neurological signs.¹⁹ In agreement with studies in patients with severe malaria,^{11–13} increased VWF:Ag levels were also observed in our MA-ARDS model suggesting that the ECs are activated during infection. This increase in plasma VWF:Ag levels occurred before parasites prominently appeared on blood smears, which is in concordance with a study in human volunteers infected with *P falciparum*.¹⁶ Reductions of plasma ADAMTS13:Act levels were also reported in patients with severe malaria.^{11,14,37} In line with these patient studies, we found that ADAMTS13:Act levels were significantly reduced at the late stage of pulmonary pathology regardless of ADAMTS13 protein levels, meaning that the reductions of ADAMTS13:Act levels might result from inhibition of ADAMTS13:Act rather than from protein loss. Potential

inhibitors of ADAMTS13 include thrombin, plasmin, interleukin-6, thrombospondin 1, free plasma hemoglobin, and FVIII, although the latter four were reported not to be associated with ADAMTS13 inhibition in patients with severe malaria.^{37–41}

A number of studies demonstrated that severe *P falciparum* malaria is associated with accumulation of ULVWF multimers in plasma.^{14,37,42} Interestingly, such an accumulation of ULVWF multimers was not visible our MA-ARDS study. In contrast, a reduction of HMW VWF multimers was observed at the end stage of disease (Figure 2). This reduction is reminiscent of what is observed in patients with type 2A von Willebrand disease, in which the deficiency of HMW VWF multimers can be caused by an increased sensitivity of plasma VWF multimers to ADAMTS13 cleavage or by mutations resulting in impaired biosynthesis of large VWF multimers.⁴³ Here, we have revealed that the loss of HMW VWF multimers following *PbNK65* infection still occurs in the absence of ADAMTS13. Plasmin has been proposed to degrade platelet-VWF complexes on ECs in

the absence of ADAMTS13²⁹; however, we showed that plasmin was also not responsible for the reduction of HMW VWF multimers. Clearly, the absence of HMW VWF multimers in experimental MA-ARDS is not caused by an increased sensitivity of VWF multimers to cleavage by ADAMTS13 or plasmin proteolysis. Coagulation abnormalities at the end stage of disease resulting in excessive consumption of HMW VWF multimers could possibly explain this reduction because disseminated intravascular coagulation is often involved with acute pulmonary insufficiency in malaria and possibly lead to the formation of fibrin clots in the lungs.⁴⁴ Future studies assessing coagulopathy and its pathophysiologic mechanisms in MA-ARDS would therefore be of interest.

Given the potential roles of VWF in promoting platelet binding and aggregation, together with several studies showing that platelets play critical roles in malaria pathogenesis,^{18,45,46} the increases in plasma VWF levels in severe malaria patients and experimental MA-ARDS raised the intriguing possibility that VWF may directly modulate the pathogenesis of MA-ARDS. Here, we demonstrate that *Vwf*^{-/-} mice have a shorter survival time than *Vwf*^{+/+} mice following *PbNK65* infection. This rapid mortality was not explained by lung edema because reduced alveolar leakage was also observed in *Vwf*^{-/-} mice. A similar discrepancy between the effects of *Vwf*^{-/-} on survival vs barrier permeability was also reported in animal models associated with increased blood-brain barrier (BBB) permeability: hypoxia/reoxygenation and pilocarpine-induced status epilepticus.⁴⁷ The authors demonstrated that reduced BBB permeability in *Vwf*^{-/-} mice was not associated with a better outcome. In contrast, all *Vwf*^{-/-} mice died during the course of the disease, whereas a large majority of *Vwf*^{+/+} mice survived.⁴⁷ Interestingly, in a mouse model of experimental cerebral malaria (ECM), *Vwf*^{-/-} mice showed attenuated BBB permeability and a prolonged survival time.⁴⁸ The attenuated BBB permeability is somehow similar to the decreased alveolar edema that we observe in our MA-ARDS model; however, the prolonged survival time observed in the ECM model could not be confirmed in our MA-ARDS model. Possibly, divergence in pathophysiology between ECM and MA-ARDS and microenvironment dissimilarity between the brain and lung could account for these differences.

Thrombocytopenia is a common feature in patients with severe malaria^{31,49} and has been ascribed to a number of mechanisms, including sequestration and enhanced clearance by macrophages in the spleen.⁵⁰ Although, previous studies have proposed that VWF might be an important modulator of malaria-associated thrombocytopenia by contributing to this enhanced platelet clearance,^{16,17,32} we observed severe thrombocytopenia in both *Vwf*^{-/-} and *Vwf*^{+/+} mice following *PbNK65* infection. This observation is in agreement with a study in ECM, where no differences in platelet count between *Vwf*^{-/-} and *Vwf*^{+/+} mice were reported.⁴⁸ These data suggest that malaria-associated thrombocytopenia is VWF independent and does not contribute to the survival difference between *Vwf*^{-/-} and *Vwf*^{+/+} mice following *PbNK65* infection.

Lovegrove et al⁵¹ revealed that high parasite levels, both overall and specifically in the lung tissue, were associated with the severity of acute lung injury induced by malaria infection. In this study, we

show that parasite load in *PbNK65*-infected *Vwf*^{-/-} mice was markedly elevated in both peripheral blood and lung tissue, which might ultimately induce malarial anemia. Although *Vwf*^{-/-} mice were protected against severe alveolar leakage, anemia together with a large increase in parasite load possibly contributed to rapid mortality following *PbNK65* infection.

Reticulocytes are immature RBCs, characterized by a reticular network formed by residual RNA.⁵² In humans, these cells represent approximately 1%-2% of circulating RBCs, whereas between 1% and 6% can be observed in mice because of the shorter lifespan of their RBCs compared with human.⁵³ *P. vivax*, one of the main *Plasmodium* species causing human malaria, is restricted to reticulocytes for its growth. Consequently, the parasitemia levels of this species are lower than species that also invade normocytes, such as *P. falciparum*. The rodent malaria species, *P. berghei* has a clear preference for invading reticulocytes over mature RBCs, but can switch to normocytes when insufficient reticulocytes are available.^{33,34,54} Our current study reveals that *Vwf*^{-/-} mice promoted increased reticulocyte production after *PbNK65* infection, leading to elevated parasitemia levels. It is unclear whether high reticulocyte production is either beneficial or harmful to the host because it could either boost parasitemia levels or serve to alleviate anemia. A number of studies in which reticulocyte production in *P. berghei*-infected rodents and *Plasmodium chabaudi*-infected mice is manipulated, however, has shown that an increase in reticulocyte production at an early stage of the infection increased parasitemia levels and reduced survival rate.⁵⁵⁻⁵⁷ Moreover, Cromer and colleagues nicely developed a mathematical model showing that suppression of reticulocyte production may in fact be advantageous to the host.⁵⁸ Possible mechanisms through which VWF deficiency is associated with increased reticulocyte production following *PbNK65* infection are still unclear. Although no overt bleeding was observed in VWF knockout mice, microbleeds could be one possibility.

Some limitations of this study need to be addressed. Most importantly, we use an experimental mouse model of MA-ARDS. Although this MA-ARDS model displays a high degree of similarity with human MA-ARDS,¹⁹ translation of our findings to human pathology should be done with caution. Parasitemia levels, for example, are relatively high in our animals and are not always detected in MA-ARDS patients, who sometimes develop MA-ARDS after the parasites are cleared by antimalarial treatment.^{59,60} Such distinctions between mouse and human pathophysiology can possibly also account for the fact that the increase of VWF:Ag in our experiments was less pronounced than that observed in patients with severe malaria, or for the fact that we did not observe a decrease in ADAMTS13:Ag, which has been reported in patients.^{11,14,37}

In conclusion, our data demonstrate that experimental MA-ARDS is associated with early elevated levels of plasma VWF and decreased levels of ADAMTS13 activity, which are in accordance with patient studies. Reduction of HMW VWF multimers was observed independently of ADAMTS13 and plasmin cleavage. In addition, malaria-associated

thrombocytopenia occurred via a VWF-independent mechanism. Increased parasite load and malarial anemia likely contribute to the shortened survival in *Vwf*^{-/-} mice, rather than alveolar leakage. Finally, we found that VWF deficiency is associated with elevated reticulocyte production following malaria infection, which leads to an increase in parasite load.

ACKNOWLEDGEMENTS

This study was supported by the Research Foundation-Flanders (FWO-Vlaanderen, project G086215N to P. E. Van den Steen and G070315 to S. F. De Meyer) and the Research Fund (C1 project C16/17/010 to P.E. Van den Steen) of the KU Leuven. K. Martinod is the recipient of a Horizon 2020 Marie Skłodowska-Curie Actions Individual Fellowship (747993). T. T. Pham holds an aspirant PhD fellowship of the FWO-Vlaanderen and P. E. Van den Steen is a Research Professor at the KU Leuven. The funders had no role in study design, data collection and analysis, decision to publish, or preparation of the manuscript.

CONFLICT OF INTERESTS

The authors state that they have no conflict of interest.

AUTHOR CONTRIBUTIONS


S. Kraisin, S. Verhenne, and S. F. De Meyer acquired, analyzed, and interpreted the data. S. Kraisin and S. F. De Meyer wrote the manuscript. S. F. De Meyer supervised and designed the study. P. E. Van den Steen provided parasites, essential protocols, cosupervised the study, and critically revised the manuscript. T.T. Pham, K. Martinod, and C. Tersteeg performed experiments, analyzed data, and revised the manuscript. N. Vandeputte performed experiments. H. Deckmyn critically revised the manuscript. K. Vanhoorelbeke cosupervised and critically revised the manuscript.

ORCID

Kimberly Martinod  <https://orcid.org/0000-0002-1026-6107>

Hans Deckmyn  <https://orcid.org/0000-0003-3952-5501>

Karen Vanhoorelbeke  <https://orcid.org/0000-0003-2288-8277>

Philippe E. Van den Steen  <https://orcid.org/0000-0002-7334-9145>

Simon F. De Meyer  <https://orcid.org/0000-0002-1807-5882>

REFERENCES

- World Health Organization. World malaria report 2017. Geneva: Switzerland; 2018.
- Barber BE, William T, Grigg MJ, Menon J, Auburn S, Marfurt J, et al. A prospective comparative study of knowlesi, falciparum, and vivax malaria in Sabah, Malaysia: high proportion with severe disease from *Plasmodium knowlesi* and *Plasmodium vivax* but no mortality with early referral and artesunate therapy. *Clin Infect Dis*. 2013;56:383-97.
- Taylor WRJ, Hanson J, Turner GDH, White NJ, Dondorp AM. Respiratory manifestations of malaria. *Chest*. 2012;142:492-505.
- Van den Steen PE, Deroost K, Deckers J, Van Herck E, Struyf S, Opdenakker G. Pathogenesis of malaria-associated acute respiratory distress syndrome. *Trends Parasitol*. 2013;29:346-58.
- O'Sullivan JM, Preston RJS, O'Regan N, O'Donnell JS. Emerging roles for hemostatic dysfunction in malaria pathogenesis. *Blood*. 2016;127:2281-8.
- Lenting PJ, Christophe OD, Denis CV. von Willebrand factor biosynthesis, secretion, and clearance: connecting the far ends. *Blood*. 2015;125:2019-28.
- Kawecki C, Lenting PJ, Denis CV. von Willebrand factor and inflammation. *J Thromb Haemost*. 2017;15:1285-94.
- Bryckaert M, Rosa J-P, Denis CV, Lenting PJ. Of von Willebrand factor and platelets. *Cell Mol Life Sci*. 2015;72:307-26.
- Mayadas TN, Johnson RC, Rayburn H, Hynes RO, Wagner DD. Leukocyte rolling and extravasation are severely compromised in P selectin-deficient mice. *Cell*. 1993;74:541-54.
- Denis CV, Andre P, Saffaripour S, Wagner DD. Defect in regulated secretion of P-selectin affects leukocyte recruitment in von Willebrand factor-deficient mice. *Proc Natl Acad Sci USA*. 2001;98:4072-7.
- Lowenberg EC, Charunwatthana P, Cohen S, van den Born B-J, Meijers JCM, Yunus EB, et al. Severe malaria is associated with a deficiency of von Willebrand factor cleaving protease, ADAMTS13. *Thromb Haemost*. 2010;103:181-7.
- Phiri HT, Bridges DJ, Glover SJ, van Mourik JA, de Laat B, M'baya B, et al. Elevated plasma von Willebrand factor and propeptide levels in Malawian children with malaria. *PLoS One*. 2011;6:e25626.
- Conroy AL, Phiri H, Hawkes M, Glover S, Mallewa M, Seydel KB, et al. Endothelium-based biomarkers are associated with cerebral malaria in Malawian children: a retrospective case-control study. *PLoS One*. 2010;5:e15291.
- de Mast Q, Groot E, Asih PB, Syafruddin D, Oosting M, Sebastian S, et al. ADAMTS13 deficiency with elevated levels of ultra-large and active von Willebrand factor in *P. falciparum* and *P. vivax* malaria. *Am J Trop Med Hyg*. 2009;80:492-8.
- Hollestelle MJ, Donkor C, Mantey EA, Chakravorty SJ, Craig A, Akoto AO, et al. von Willebrand factor propeptide in malaria: evidence of acute endothelial cell activation. *Br J Haematol*. 2006;133:562-9.
- de Mast Q, Groot E, Lenting PJ, de Groot PG, McCall M, Sauerwein RW, et al. Thrombocytopenia and release of activated von Willebrand factor during early *Plasmodium falciparum* malaria. *J Infect Dis*. 2007;196:622-8.
- de Mast Q, de Groot PG, van Heerde WL, Roestenberg M, van Velzen JF, Verbruggen B, et al. Thrombocytopenia in early malaria is associated with GP1b shedding in absence of systemic platelet activation and consumptive coagulopathy. *Br J Haematol*. 2010;151:495-503.
- Bridges DJ, Bunn J, van Mourik JA, Grau G, Preston RJS, Molyneux M, et al. Rapid activation of endothelial cells enables *Plasmodium falciparum* adhesion to platelet-decorated von Willebrand factor strings. *Blood*. 2010;115:1472-4.
- Van den Steen PE, Geurts N, Deroost K, Van Aelst I, Verhenne S, Heremans H, et al. Immunopathology and dexamethasone therapy in a new model for malaria-associated acute respiratory distress syndrome. *Am J Respir Crit Care Med*. 2010;181:957-68.
- Vandermosten L, Pham T-T, Possemiers H, Knoops S, Van Herck E, Deckers J, et al. Experimental malaria-associated acute respiratory distress syndrome is dependent on the parasite-host combination and coincides with normocyte invasion. *Malar J*. 2018;17:102.

21. Denis C, Methia N, Frenette PS, Rayburn H, Ullman-Cullere M, Hynes RO, et al. A mouse model of severe von Willebrand disease: defects in hemostasis and thrombosis. *Proc Natl Acad Sci USA*. 1998;95:9524-9.
22. Verhenne S, Denorme F, Libbrecht S, Vandenbulcke A, Pareyn I, Deckmyn H, et al. Platelet-derived VWF is not essential for normal thrombosis and hemostasis but fosters ischemic stroke injury in mice. *Blood*. 2015;126:1715-22.
23. De Meyer SF, Vandeputte N, Pareyn I, Petrus I, Lenting PJ, Chuah MKL, et al. Restoration of plasma von Willebrand factor deficiency is sufficient to correct thrombus formation after gene therapy for severe von Willebrand disease. *Arterioscler Thromb Vasc Biol*. 2008;28:1621-6.
24. Deforche L, Tersteeg C, Roose E, Vandenbulcke A, Vandeputte N, Pareyn I, et al. Generation of anti-murine ADAMTS13 antibodies and their application in a mouse model for acquired thrombotic thrombocytopenic purpura. *PLoS One*. 2016;11:e0160388.
25. De Cock E, Hermans C, De Raeymaecker J, De Ceunynck K, De Maeyer B, Vandeputte N, et al. The novel ADAMTS13-p.D187H mutation impairs ADAMTS13 activity and secretion and contributes to thrombotic thrombocytopenic purpura in mice. *J Thromb Haemost*. 2015;13:283-92.
26. Lijnen HR, Van Hoef B, Dewerchin M, Collen D. Alpha(2)-antiplasmin gene deficiency in mice does not affect neointima formation after vascular injury. *Arterioscler Thromb Vasc Biol*. 2000;20:1488-92.
27. Tersteeg C, Joly BS, Gils A, Lijnen R, Deckmyn H, Declerck PJ, et al. Amplified endogenous plasmin activity resolves acute thrombotic thrombocytopenic purpura in mice. *J Thromb Haemost*. 2017;15:2432-42.
28. Livak KJ, Schmittgen TD. Analysis of relative gene expression data using real-time quantitative PCR and the 2(-Delta Delta C(T)) method. *Methods*. 2001;25:402-8.
29. Tersteeg C, de Maat S, De Meyer SF, Smeets MWJ, Barendrecht AD, Roest M, et al. Plasmin cleavage of von Willebrand factor as an emergency bypass for ADAMTS13 deficiency in thrombotic microangiopathy. *Circulation*. 2014;129:1320-31.
30. Tersteeg C, Schiviz A, De Meyer SF, Plaimauer B, Scheifflinger F, Rottensteiner H, et al. Potential for recombinant ADAMTS13 as an effective therapy for acquired thrombotic thrombocytopenic purpura. *Arterioscler Thromb Vasc Biol*. 2015;35:2336-42.
31. Cox D, McConkey S. The role of platelets in the pathogenesis of cerebral malaria. *Cell Mol Life Sci*. 2010;67:557-68.
32. Schwameis M, Schorghofer C, Assinger A, Steiner MM, Jilma B. VWF excess and ADAMTS13 deficiency: a unifying pathomechanism linking inflammation to thrombosis in DIC, malaria, and TTP. *Thromb Haemost*. 2015;113:708-18.
33. Deharo E, Coquelin F, Chabaud AG, Landau I. The erythrocytic schizogony of two synchronized strains of *Plasmodium berghei*, NK65 and ANKA, in normocytes and reticulocytes. *Parasitol Res*. 1996;82:178-82.
34. Cromer D, Evans KJ, Schofield L, Davenport MP. Preferential invasion of reticulocytes during late-stage *Plasmodium berghei* infection accounts for reduced circulating reticulocyte levels. *Int J Parasitol*. 2006;36:1389-97.
35. Yoeli M, Upmanis RS, Vanderberg J, Most H. Life cycle and patterns of development of *Plasmodium berghei* in normal and experimental hosts. *Mil Med*. 1966;131(Suppl):900-14.
36. Wiczling P, Krzyzanski W. Flow cytometric assessment of homeostatic aging of reticulocytes in rats. *Exp Hematol*. 2008;36:119-27.
37. Larkin D, de Laat B, Jenkins PV, Bunn J, Craig AG, Terraube V, et al. Severe *Plasmodium falciparum* malaria is associated with circulating ultra-large von Willebrand multimers and ADAMTS13 inhibition. *PLoS Pathog*. 2009;5:e1000349.
38. Bernardo A, Ball C, Nolasco L, Moake JF, Dong J. Effects of inflammatory cytokines on the release and cleavage of the endothelial cell-derived ultralarge von Willebrand factor multimers under flow. *Blood*. 2004;104:100-6.
39. Kremer Hovinga JA, Antoine G, Hermann M, Rieger M, Scheifflinger F, Lammler B, et al. Fatal congenital thrombotic thrombocytopenic purpura with apparent ADAMTS13 inhibitor: in vitro inhibition of ADAMTS13 activity by hemoglobin. *Blood*. 2005;105:542-4.
40. Bonnefoy A, Daenens K, Feys HB, De Vos R, Vandervoort P, Vermylen J, et al. Thrombospondin-1 controls vascular platelet recruitment and thrombus adherence in mice by protecting (sub)endothelial VWF from cleavage by ADAMTS13. *Blood*. 2006;107:955-64.
41. Crawley JTB, Lam JK, Rance JB, Mollica LR, Donnell JSO, Lane DA, et al. Proteolytic inactivation of ADAMTS13 by thrombin and plasmin. *Blood*. 2005;105:1085-93.
42. Graham SM, Chen J, Chung DW, Barker KR, Conroy AL, Hawkes MT, et al. Endothelial activation, haemostasis and thrombosis biomarkers in Ugandan children with severe malaria participating in a clinical trial. *Malar J*. 2016;15:56.
43. Favaloro EJ. Appropriate laboratory assessment as a critical facet in the proper diagnosis and classification of von Willebrand disorder. *Best Pract Res Clin Haematol*. 2001;14:299-319.
44. Punyagupta S, Srichaikul T, Nitiyanant P, Petchchai B. Acute pulmonary insufficiency in falciparum malaria: summary of 12 cases with evidence of disseminated intravascular coagulation. *Am J Trop Med Hyg*. 1974;23:551-9.
45. Wassmer SC, Combes V, Candal FJ, Juhan-vague I, Grau GE. Platelets potentiate brain endothelial alterations induced by *Plasmodium falciparum* platelets potentiate brain endothelial alterations induced by *Plasmodium falciparum*. *Infect Immun*. 2006;74:645-53.
46. McMorran BJ, Marshall VM, de Graaf C, Drysdale KE, Shabbar M, Smyth GK, et al. Platelets kill intraerythrocytic malarial parasites and mediate survival to infection. *Science*. 2009;323:797-800.
47. Suidan GL, Brill A, De Meyer SF, Voorhees JR, Cifuni SM, Cabral JE, et al. Endothelial von Willebrand factor promotes blood-brain barrier flexibility and provides protection from hypoxia and seizures in mice. *Arterioscler Thromb Vasc Biol*. 2013;33:2112-20.
48. O'Regan N, Gegenbauer K, O'Sullivan JM, Maleki S, Brophy TM, Dalton N, et al. A novel role for von Willebrand factor in the pathogenesis of experimental cerebral malaria. *Blood*. 2016;127:1192-201.
49. Faille D, El-Assaad F, Alessi M-C, Fusai T, Combes V, Grau GE. Platelet-endothelial cell interactions in cerebral malaria: the end of a cordial understanding. *Thromb Haemost*. 2009;102:1093-102.
50. Lacerda MVG, Mourao MPG, Coelho HCC, Santos JB. Thrombocytopenia in malaria: who cares? *Mem Inst Oswaldo Cruz*. 2011;106(Suppl):52-63.
51. Lovegrove FE, Gharib SA, Peña-Castillo L, Patel SN, Ruzinski JT, Hughes TR, et al. Parasite burden and CD36-mediated sequestration are determinants of acute lung injury in an experimental malaria model. *PLoS Pathog*. 2008;4.
52. Orten JM. The properties and significance of the reticulocyte. *Yale J Biol Med*. 1934;6:519-39.
53. Everds N. Hematology of the laboratory mouse A. In: MT Davisson, FW Quimby, SW Barthold, CE Newcomer, A Smith, editors. *The mouse in biomedical research (Second Edition)*. Waltham: Academic Press, 2007; p. 133-70.
54. Butcher GA, Mitchell GH, Cohen S. Letter: mechanism of host specificity in malarial infection. *Nature*. 1973;244:40-1.
55. Singer I. The course of infection with *Plasmodium berghei* in inbred CF 1 mice. *J Infect Dis*. 1954;94:237-40.
56. Chang K-H, Tam M, Stevenson MM. Modulation of the course and outcome of blood-stage malaria by erythropoietin-induced reticulocytosis. *J Infect Dis*. 2004;189:735-43.

57. Zuckerman A. Blood loss and replacement in plasmodial infections. I. *Plasmodium berghei* in untreated rats of varying age and in adult rats with erythropoietic mechanisms manipulated before inoculation. *J Infect Dis.* 1957;100:172-206.
58. Cromer D, Stark J, Davenport MP. Low red cell production may protect against severe anemia during a malaria infection—insights from modeling. *J Theor Biol.* 2009;257:533-42.
59. Habib AG, Singh KS. Respiratory distress in nonimmune adults with imported malaria. *Infection.* 2004;32:356-9.
60. Tanius MA, Kogelman L, McGovern B, Hassoun PM. Acute respiratory distress syndrome complicating *Plasmodium vivax* malaria. *Crit Care Med.* 2001;29:665-7.

SUPPORTING INFORMATION

Additional supporting information may be found online in the Supporting Information section at the end of the article.

How to cite this article: Kraisin S, Verhenne S, Pham T-T, et al. von Willebrand factor in experimental malaria-associated acute respiratory distress syndrome. *J Thromb Haemost.* 2019;17:1372-1383. <https://doi.org/10.1111/jth.14485>